JACS
JOURNAL OF THE AMERICAN CHEMICAL SOCIETY

Article

pubs.acs.org/JACS

Scope and Mechanism in Palladium-Catalyzed Isomerizations of Highly Substituted Allylic, Homoallylic, and Alkenyl Alcohols

Evgeny Larionov,[†] Luqing Lin,[†] Laure Guénée,[‡] and Clément Mazet*[,†]

[†]Department of Organic Chemistry, University of Geneva, 30 quai Ernest Ansermet, 1211 Geneva, Switzerland

[‡]Laboratory of Crystallography, University of Geneva, 24 quai Ernest Ansermet, 1211 Geneva, Switzerland

Supporting Information

ABSTRACT: Herein we report the palladium-catalyzed isomerization of highly substituted allylic alcohols and alkenyl alcohols by means of a single catalytic system. The operationally simple reaction protocol is applicable to a broad range of substrates and displays a wide functional group tolerance, and the products are usually isolated in high chemical yield. Experimental and computational mechanistic investigations provide complementary and converging evidence for a chain-walking process consisting of repeated migratory insertion/β-H elimination sequences. Interestingly, the catalyst does not dissociate from the substrate in the isomerization of allylic alcohols, whereas it disengages during the isomerization of alkenyl alcohols when additional substituents are present on the alkyl chain.

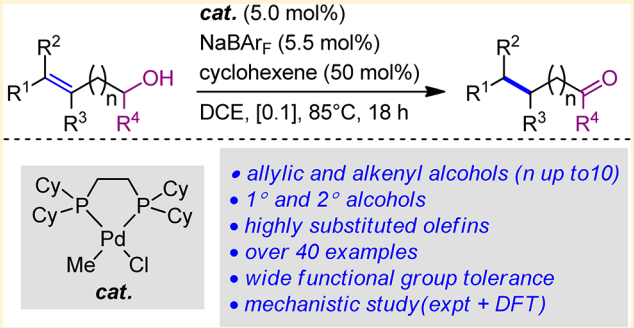

INTRODUCTION

Driven by the contemporary needs of developing sustainable processes, the efficiency of a chemical reaction is no longer a simple measure of its yield, but fundamental principles such as atom economy, step economy, and redox economy have become primary concerns.[1,2] In order to readily access elaborated structures, the notion of rapid increase in molecular complexity has been paralleling these concepts, leading to the design of novel catalytic and selective reactions.[3] Consequently, cascade, tandem, and isomerization reactions have attracted renewed interest because they reduce oxidation/reduction sequences, protection/deprotection events, and functional group manipulations while streamlining access to more complex target molecules.

Metal-catalyzed directed isomerizations of functionalized olefins are particularly attractive because, upon migration of a C=C bond, the substrates undergo *refunctionalization* in an overall redox-neutral operation with no chemical waste generated.[4,5] Among some of the most relevant examples, the Rh-catalyzed enantioselective isomerization of allylic amines to chiral enamines constitutes a notorious illustration of the potential of a nearly perfect isomerization.[6] Over 30 years ago, joint efforts from academia and industry resulted in the development of an extraordinarily active and enantioselective rhodium catalyst for the quantitative isomerization of *N,N*-dialkylgeranylamine derivatives with excellent regioselectivity and perfect enantioselectivity. The use of extremely low loadings of a recyclable catalyst under mild reaction conditions enabled its implementation as the key step in the industrial production of menthol, the world's best-selling aroma ingredient. These achievements are undoubtedly formidable but unfortunately mask the numerous challenges that still remain in the field of transition-metal-catalyzed isomerizations of analogous allylic systems.

Even though some useful progress has been made, the seemingly related isomerization of allylic alcohols has not reached the same level of refinement (Figure 1A).[5] Recent advances include the discovery of Ru, Rh, and Ir catalysts for the isomerization of primary and secondary allylic alcohols under relatively mild reaction conditions. Concomitantly, efforts have also been directed toward the development of enantioselective variants of these isomerizations, mostly with primary allylic alcohols. Notable examples from the Fu group (Rh),[7] our group (Ir),[8] and more recently Okhuma and co-workers (Ru)[9] are worth mentioning. Examples of asymmetric isomerization of secondary allylic alcohols are rare.[10] Unfortunately, all of these systems—whether enantioselective or not—are usually very substrate-specific, and to date there is *no general catalyst* for the isomerization of both primary and secondary allylic alcohols. It is usually admitted that a direct correlation exists between the degree of substitution of the C=C bond and the difficulty associated with the isomerization of allylic alcohols.[5] Substrates with more-substituted double bonds are less reactive, as schematically shown in Figure 1B. This trend is explained by the fact that it is difficult for transition-metal complexes to bind and react with heavily substituted olefins, and not surprisingly, isomerizations of allylic alcohols with a tetrasubstituted double bond are very rare.[8a,f] Therefore, it is widely appreciated that further developments will benefit

Received: August 25, 2014
Published: November 14, 2014

   dx.doi.org/10.1021/ja508736u | J. Am. Chem. Soc. 2014, 136, 16882−16894

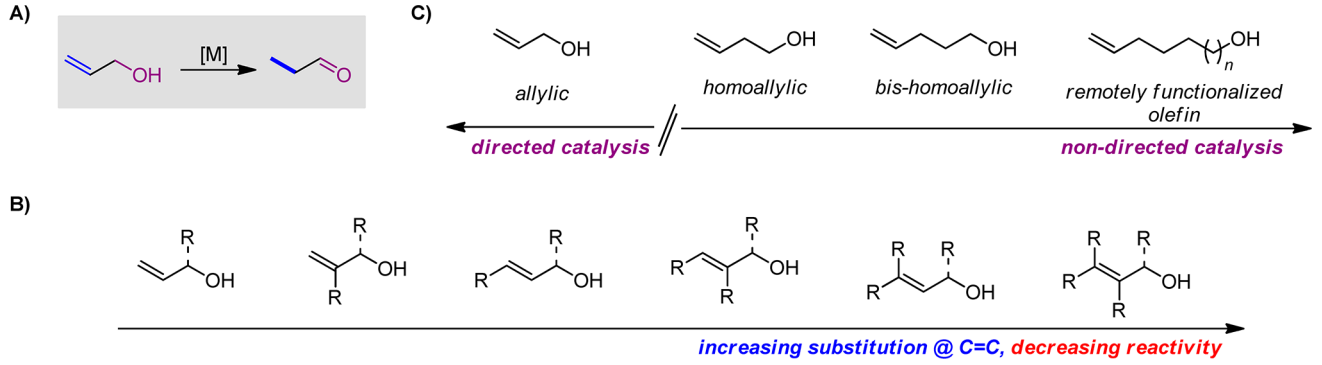

Figure 1. (A) Challenges in allylic and alkenyl alcohol isomerizations. (B) Reactivity as a function of olefin substitution pattern. It should be noted that no catalyst is currently effective for a breadth of both primary and secondary allylic alcohols. (C) Bridging the gap between "biased" allylic alcohols and remote homo-, bis-homo-, and alkenyl alcohols.

from the discovery of a more general catalyst that would indifferently isomerize primary and secondary allylic alcohols independently of the extent of substitution of the olefinic moiety.

Interestingly, none of the Ru, Rh, or Ir catalysts mentioned above is able to isomerize homoallylic alcohols, bis-homoallylic alcohols, or more remote alkenyl alcohols. This clearly indicates that the hydroxyl directing group plays a crucial role in imparting catalytic activity, independently of the mechanistic subtleties that distinguish these systems. In 2007, Grotjhan and co-workers reported a bifunctional Ru catalyst for the long-range migration of unhindered double bonds (up to 30 units).[11] The substrate scope included several examples of primary and secondary alkenyl alcohols with a terminal C=C bond that were converted into the corresponding carbonyl derivatives. Of note, when geraniol was subjected to the optimized reaction conditions, the homoallylic alcohol (*E*)-*iso*-geraniol rather than citronellal was generated in 61% yield. To our knowledge, catalysts that can perform the isomerization of both allylic and alkenyl alcohols are scarce; they are limited to unhindered terminal or disubstituted double bonds, and the yields of the products are usually low or moderate.[5−10,12]

The propensity of Pd catalysts to migrate C=C bonds over several positions by the so-called zipper or chain-walking process was first exploited in the context of olefin polymerization.[13] Recently, several groups have capitalized on this ability in more synthetic-oriented settings. Relevant examples include the catalytic cycloisomerization of various 1,*n*-dienes by Kochi and co-workers.[14] Their approach allows the formation of five-membered rings by facile C−C bond formation upon isomerization of a double bond and intramolecular interception of a cyclohexene moiety. However, it is applicable only to substrates with a terminal olefin, which facilitates the first insertion of the putative palladium hydride intermediate. Gooßen and co-workers have developed an isomerizing olefin metathesis for the conversion of fatty acids (i.e., substrates with an internal disubstituted double bond) into dicarboxylic acids of adjustable chain lengths.[15] The system relies on the successful combination of a Pd isomerization catalyst and the Grubbs ruthenium metathesis catalyst. In a remarkable series of papers, Sigman and co-workers have described highly enantioselective redox-relay Heck arylations of acyclic alkenyl alcohols.[16] Using either aryl diazonium salts (Heck−Matsuda) or boronic acid derivatives (oxidative Heck), the methods provide access to remotely functionalized arylated carbonyls. When trisubstituted olefins are employed, the preferred site selectivity for the more hindered position enables the formation of quaternary stereocenters with high enantioselectivity. Despite these formidable achievements, the oxidative conditions employed and the strong influence of both coupling partners on the regioselectivity of the initial migratory insertion are current limitations of the approach.

As part of our program directed toward the discovery of well-defined transition-metal hydrides for isomerization reactions,[8,9] we recently disclosed a novel [Pd−H] catalyst for the selective rearrangement of di- and trisubstituted epoxides into aldehydes and ketones.[17] Computational and experimental studies pointed to an unusual addition/elimination mechanism reminiscent of the typical sequence usually proposed for alkene migrations.[18] This finding and the ability of Pd catalysts to sustain olefin migration along extended carbon chains (vide supra) motivated us to identify a well-defined catalyst that would isomerize both primary and secondary allylic alcohols as well as alkenyl alcohols independently of the olefinic substitution pattern. If successful, such a system would bridge the gap between directed and nondirected isomerizations and certainly complement existing synthetic alternatives (Figure 1C).

In this article, we describe our progress toward achieving this goal, specifically a functional-group-tolerant catalytic system that can isomerize a variety of substrates. Furthermore, our study provides detailed mechanistic information obtained by a combined experimental and theoretical approach.

RESULTS AND DISCUSSION

Reaction Optimization. The system initially reported for the isomerization of epoxides employed the well-defined dinuclear palladium complex $[(dippp)_3(Pd{-}H)_2)](OTf)_2$ **1** (dippp = 1,3-bis(diisopropylphosphino)propane).[17] For our initial investigations, we chose to explore the isomerization of four distinct geometrically pure substrates: the trisubstituted primary allylic alcohol (*E*)-**2a**, the disubstituted secondary allylic alcohol (*E*)-**2b**, and the di- and trisubstituted homoallylic alcohols (*E*)-**4b** and (*E*)-**4c**, respectively. The reactions were conducted under conditions similar to those employed for the isomerization of epoxides (5 mol % [Pd], 85 °C, 18 h), but tetrahydrofuran was replaced by 1,2-dichloroethane (DCE), a less-coordinating solvent. Productive isomerizations of substrates (*E*)-**2b**, (*E*)-**4b**, and (*E*)-**4c** were observed, and the desired carbonyl compounds **3b**, **5b**, and **5c** were isolated in 62%, 66%, and 40% yield, respectively. The remainder was essentially the unreacted starting material in all cases. In

dx.doi.org/10.1021/ja508736u | J. Am. Chem. Soc. 2014, 136, 16882−16894

contrast, isomerization of (*E*)-**2a** led to a mixture of aldehyde **3a**, (*Z*)-**2a**, and the corresponding homoallylic alcohol with a terminal olefin, **4a** (Scheme 1). The disparate results obtained

Scheme 1. Isomerization of Representative Substrates by Complex 1

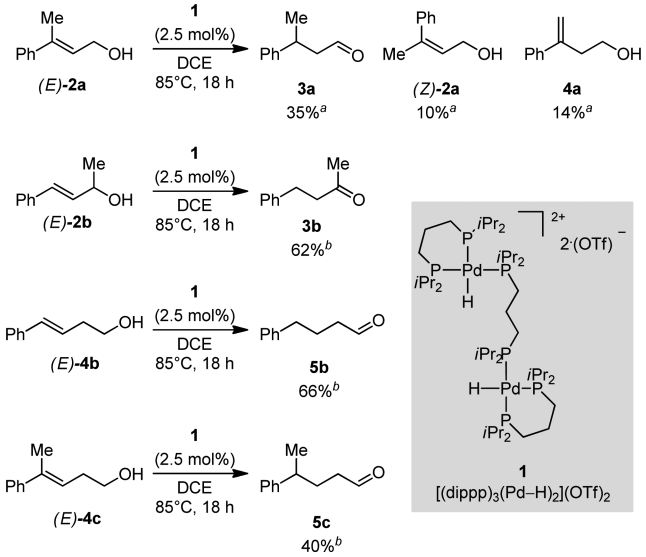

[a]Conversion determined by ^{1}H NMR analysis of the crude reaction mixture. [b]Yield after chromatography.

for the isomerization of (*E*)-**2a** and (*E*)-**4c** already suggest the existence of (subtle) mechanistic differences for the isomerization of highly substituted allylic and homoallylic alcohols.

To circumvent this selectivity issue and in order to identify a more general catalyst, we set out to explore the influence of the supporting ligand on the outcome of these reactions. Unfortunately, attempts to synthesize and isolate [Pd–H] analogues of **1** with other chelating ligands (such as **6**, **8**, or **10**) were not successful. Inspired by precedents in olefin polymerization[13] and by the work of Kochi and co-workers,[14] we turned our attention to the synthesis of neutral palladium complexes of general formula [L_nPd(Me)(Cl)] where L_n is a chelating bidentate ligand. Admittedly, these species provide in situ access to the corresponding cationic hydride [L_n(Pd–H)]$^+$ by halide abstraction in the presence of a sacrificial olefin additive. The three bidentate ligands dippp (**6**), 2,2′-bipyridine (bipy, **8**), and 2-(2-(diphenylphosphino)phenyl)-4,5-dihydrooxazole (phox, **10**) were selected because of their distinct donor abilities. The ligand 1,2-bis(dicyclohexylphosphino)ethane (dcpe, **12**) was chosen because of its smaller bite angle with respect to **6**, a parameter that we anticipated might be important for tuning the hydricity of the palladium intermediate.[19] The corresponding complexes **7**, **9**, **11**, and **13** were prepared in good yields (67–86%; Scheme 2). Of note, complex **11** was obtained as a single isomer, as was apparent from ^{1}H, ^{13}C{^{1}H}, and ^{31}P{^{1}H} NMR spectroscopy. The methyl group was proposed to be located trans to the N-donor atom on the basis of the characteristic coupling constant $^3J_{PH}$ = 3.3 Hz. This was later confirmed by X-ray analysis of a single crystal of **11**. A crystal structure was also obtained for the air-stable complex **13**.

The performances of these four palladium complexes were first evaluated in the isomerizations of (*E*)-**2a** and (*E*)-**4c** using 5.5 mol % $NaBAr_F$ (BAr_F = tetrakis(3,5-bis(trifluoromethyl)-

Scheme 2. Syntheses of Complexes 7, 9, 11, and 13 Along with the X-ray Structures of 11 and 13

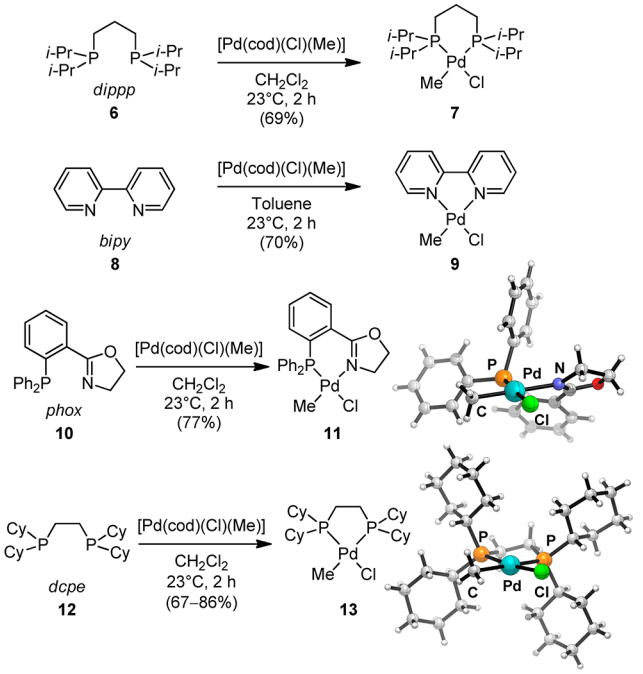

phenyl)borate) and 50 mol % cyclohexene in DCE at 85 °C for 18 h (Table 1). The two complexes supported by bisphosphine ligands resulted in complete conversion of (*E*)-**2a** into **3a** (entries 1 and 4), while the catalysts supported by the (P,N)

Table 1. Survey of Catalysts

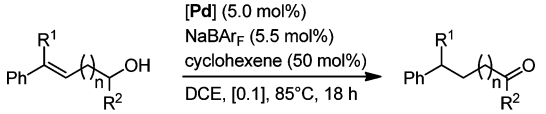

entry[a]	substrate	catalyst	cons. (%)[b]	conv. (%)[c]
1	(*E*)-**2a**	**7**	>99	96 (44)
2	(*E*)-**2a**	**9**	>99	<5[d]
3	(*E*)-**2a**	**11**	>99	<5[d]
4	(*E*)-**2a**	**13**	>99	>99 (68)
5	(*E*)-**4c**	**7**	65	16[e]
6	(*E*)-**4c**	**9**	58	<5[f]
7	(*E*)-**4c**	**11**	51	<5[g]
8	(*E*)-**4c**	**13**	93	24[h]
9	(*E*)-**2b**	**7**	80	65 (30)
10	(*E*)-**2b**	**13**	99	97 (92)
11	(*E*)-**4b**	**7**	93	71 (50)
12	(*E*)-**4b**	**13**	92	83 (70)

[a]Reactions were performed on a 0.25 mmol scale. [b]Consumption of starting material as determined by ^{1}H NMR spectroscopy using an internal standard. [c]Conversion to product as determined by ^{1}H NMR spectroscopy using an internal standard. Values in parentheses are yields after chromatography. [d]Complex reaction mixture and catalyst decomposition. [e]Along with a 9% yield of (*Z*)-**4c** and unidentified oligomeric products. [f]Along with an 8% yield of (*Z*)-**4c**, an 8% yield of the terminal bis-homoallylic alcohol, and unidentified oligomeric materials. [g]Along with a 15% yield of (*Z*)-**4c**. [h]Along with unidentified oligomeric materials.

dx.doi.org/10.1021/ja508736u | J. Am. Chem. Soc. 2014, 136, 16882–16894

and (N,N) ligands led to intractable mixtures that did not contain any traces of the product (entries 2 and 3). For homoallylic alcohol (*E*)-**4c**, the catalytic activities of **7** and **13** were substantially reduced, and **5c** was formed in 16% and 24% yield, respectively (entries 5 and 8). These reactions were accompanied by the formation of (*Z*)-**4c** and unidentified oligomeric materials.[20] No productive isomerization was detected with **9** and **11** (entries 6 and 7). In evaluating **7** and **13** further, the latter turned out to offer the best performances, as isomerization of secondary alcohol (*E*)-**2b** and homoallylic alcohol (*E*)-**4b** afforded the corresponding carbonyl derivatives **3b** and **5b** in 92% and 70% yield, respectively (entries 10 and 12). These results were not improved by additional optimization of the reaction conditions (see the Supporting Information (SI)).

From these studies, it appears that complexes **1** and **7**, which are expected to generate a common palladium hydride intermediate, give contrasting results. The former performs best for homoallylic alcohols but poorly for allylic alcohols, while the latter follows the opposite trend. Complexes **9** and **11** are poor catalysts even for the more reactive substrates. This is especially surprising for **9**, as most Pd-catalyzed long-range olefin migrations reported in the literature rely on complexes supported by (N,N) ligands.[13,14,16] Finally, the straightforward availability of **13** along with the well-balanced reactivity pattern obtained for substrates (*E*)-**2a**/**2b** and (*E*)-**4b**/**4c** prompted us to carry out further investigations with this air-stable complex.

Reaction Scope. A collection of primary and secondary allylic alcohols with a representative set of olefin substitution patterns and functional groups were synthesized and submitted to the reaction conditions (Scheme 3). Primary and secondary cinnamyl alcohols were efficiently converted to the corresponding aldehydes and ketones in moderate to excellent yields (**3b**–**j**, 62–92% yield). Allylic alcohols with a 2,3,3- or a 2,2,3-trisubstituted olefinic pattern were isomerized with similar efficiencies (**3k**–**p**, 51–94% yield; **3q** and **3r**, 90–92% yield). While steric hindrance did not affect the reaction (R^1 = *o*-ClC_6H_4, Cy; R^2 = *i*-Pr, Cy; R^4 = *i*-Pr), sensitive functional groups and heterocycles such as fluoride, chloride, bromide, methoxy, nitro, hydroxyl, and *N*-methylpyrrole were all very well tolerated. The latter example is interesting because hydride insertion occurs at a bisbenzylic position. Isomerization of a primary allylic alcohol with a tetrasubstituted olefin delivered aldehyde **3s** in 70% yield as a 1:1 mixture of cis and trans isomers. In contrast, isomerization of **2t**, a secondary allylic alcohol with a tetrasubstituted C=C bond, led to the formation of 4*H*-chromene **14** in 69% yield (Figure 2).

The exact same catalytic system was next evaluated in the isomerization of 16 different primary and secondary homoallylic alcohols **4a**–**p** (Scheme 4). Interestingly, 3-phenyl-3-butenol, a substrate with a terminal olefin, was converted into **5a** in 52% yield. This is noteworthy, as one may expect unproductive insertion of Pd at the least encumbered olefinic position to occur preferentially. Homoallylic alcohols with a disubstituted olefin were isomerized efficiently (**5b**, 70% yield; **5d**, 58% yield). Whereas **5c** was obtained in only 29% yield,[20] **4e**, **4o**, and **4p** reacted with increased efficiency (isolated yields: **5e**, 51%; **5o**, 87%; **5p**, 94%). Although we had initial concerns regarding the site-selective insertion of Pd for substrates with a 3,3,4-trisubstituted olefinic pattern (**4f**–**n**), the result obtained for **4a** prompted us to explore their reactivity. Gratifyingly, productive isomerization to the desired carbonyl derivatives was systematically observed. Homoallylic alcohols with an aromatic

Scheme 3. Isomerization of Allylic Alcohols with 13[a]

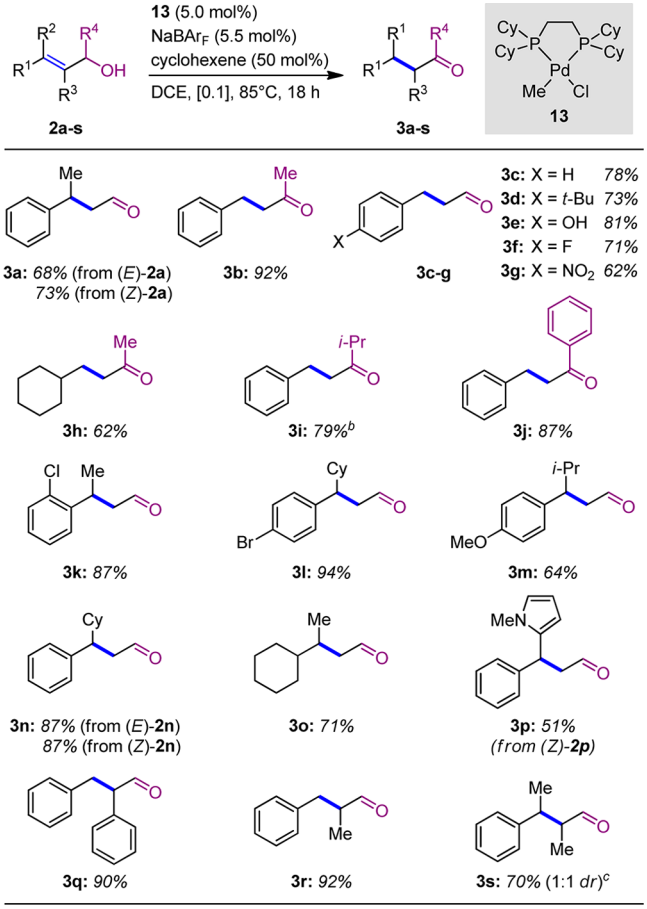

[a]Reactions were performed on a 0.25 mmol scale. The substrates were *E*-configured, unless otherwise noted. Yields after chromatography are shown. [b]On a 0.5 mmol scale. [c]With 10 mol % cyclohexene.

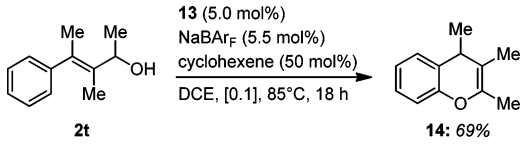

Figure 2. Tentative isomerization of **2t**, a tetrasubstituted secondary allylic alcohol.

substituent at both C3 and C4 delivered the products in moderate yields (**5f**–**5j**, 37–55% yield), while substrates with an aryl group at C4 and an alkyl substituent at C3 proved particularly suitable (**5l**–**n**, 80–89% yield). Isomerization of alkenyl alcohols with a more remote trisubstituted double bond was also successfully achieved. Thus, **5q** was isolated in 75% yield from the corresponding bis-homoallylic alcohol. Interestingly, while *rac*-citronellol was isomerized to *rac*-3,7-dimethyloctanal (*rac*-**5r**) in only 38% yield, the corresponding secondary alcohol delivered *rac*-**5s** in 71% yield. In both cases, the remainder consisted of unreacted starting material. These results are remarkable because the presence of an additional alkyl substituent along the alkyl chain does not interrupt the catalysis. These observations are in line with recent findings by Sigman and co-workers.[16d] Finally, isomerization of a terminal (**4t**) or disubstituted (**4u**) C=C bond over 11 positions afforded **5t** and **5u** in 92% and 79% yield, respectively.

dx.doi.org/10.1021/ja508736u | J. Am. Chem. Soc. 2014, 136, 16882–16894

Scheme 4. Isomerization of Homoallylic and Alkenyl Alcohols with 13[a]

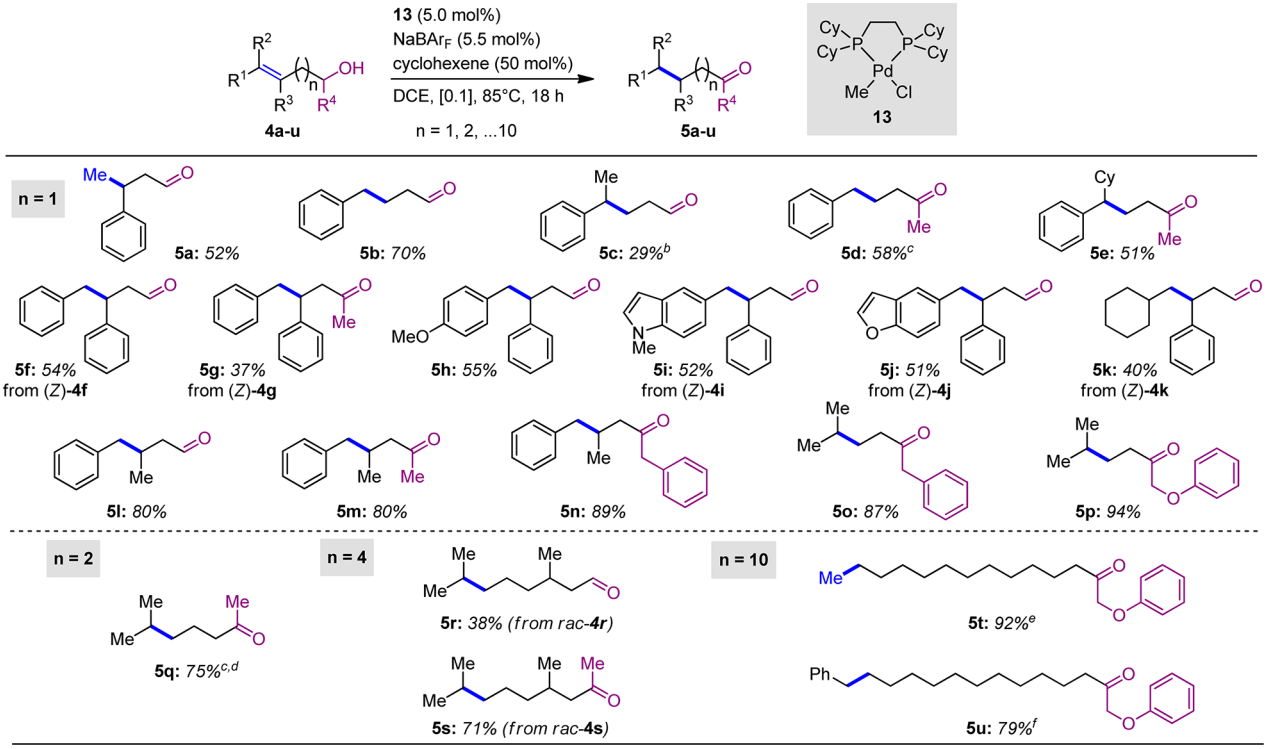

[a]Reactions were performed on a 0.25 mmol scale. Substrates were *E*-configured, unless otherwise noted. Yields after chromatography are shown. [b]Without cyclohexene. [c]48 h. [d]On a 0.75 mmol scale. [e]4 h, 93% purity. [f]On a 0.1 mmol scale.

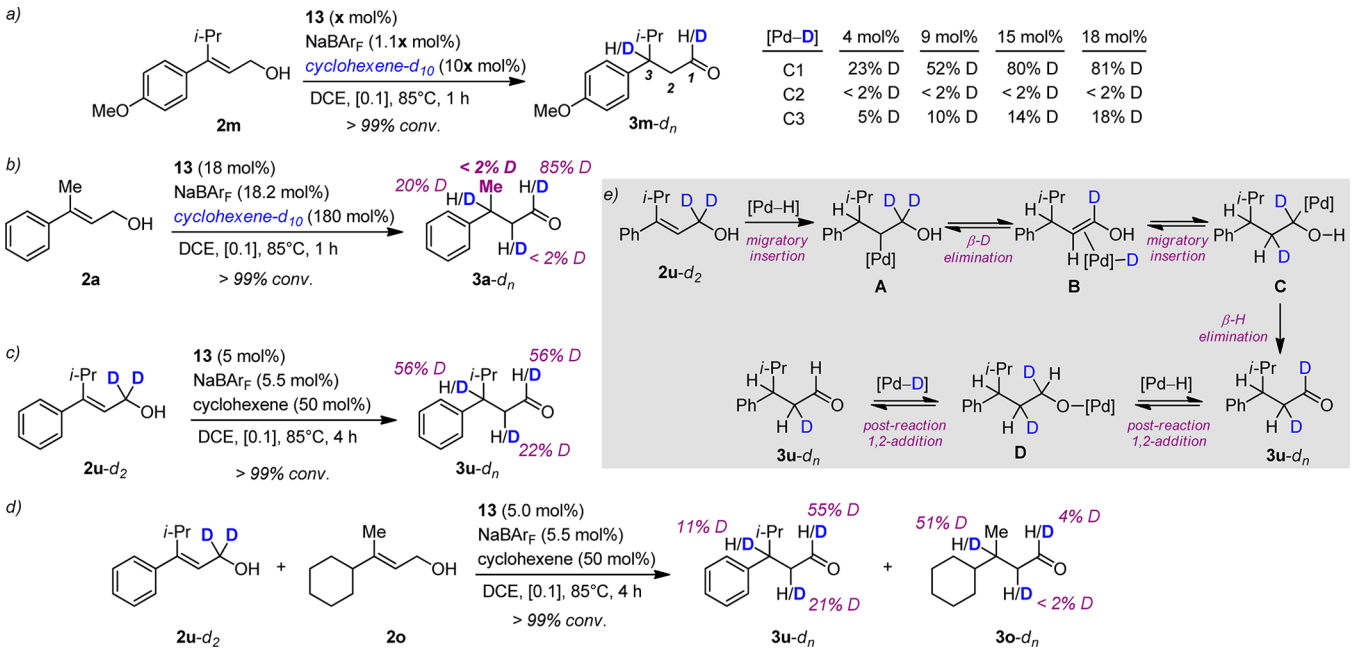

Figure 3. (a–c) Labeling experiments: (a) with **2m** and in situ generation of [Pd–D] using various Pd loadings; (b) with **2a** and in situ generation of [Pd–D]; (c) with **2u**-d_2 and in situ generation of [Pd–H]. (d) Crossover experiment. (e) Mechanistic rationale.

Mechanistic Experiments. In order to obtain preliminary insights into the reaction mechanism, a series of labeling experiments was carried out (Figure 3). First, reactions with substrate **2m** were conducted using different loadings of Pd in the presence of cyclohexene-d_{10} to generate a [Pd–D] catalyst in situ.[21] After full consumption of **2m**, ^{2}H NMR analysis of the crude reaction mixture showed that deuterium was incorporated at C1 and C3 exclusively. No incorporation at C2 was detected. Quantitative ^{1}H NMR analysis indicated that the extent of deuterium incorporation at C3 matched the initial loading of **13**, clearly establishing that the first insertion of palladium deuteride into the C=C bond is *irreversible*.[22] In contrast, deuterium scrambling at C1 is consistent with postreaction reversible insertion of palladium deuteride across

dx.doi.org/10.1021/ja508736u | J. Am. Chem. Soc. 2014, 136, 16882–16894

the C=O bond of the aldehyde (vide infra). This leads to equilibration of the [Pd−H] and [Pd−D] intermediates and accounts for the higher extent of D incorporation at C1 with respect to the initial loading of **13** (Figure 3a). When **2a** was reacted with 18 mol % **13** and a 10-fold excess of cyclohexene-d_{10}, no significant incorporation of deuterium on the methyl group was detected, suggesting that Pd inserts exclusively at C2 even for sterically less-demanding allylic alcohols (Figure 3b).

Labeling experiments employing dideuterated substrate **2u**-d_2 were carried out using the standard procedure for the in situ generation of a [Pd−H] catalyst (Figure 3c). After completion, ^{1}H and ^{2}H NMR analyses of the crude reaction mixture showed deuterium scrambling at C1, C2, and C3. Although in apparent contradiction with the experiments of Figure 3a (no D incorporation at C2), this result can be explained by reversible insertion of the [Pd−D] species into the transient enol intermediate **B**. The subsequent insertion product **C** undergoes *irreversible* β-H elimination to give aldehyde **3u**. Postreaction reinsertion of the [Pd−H] occurs preferentially by formation of the Pd−alkoxy intermediate **D** rather than the α-hydroxy Pd−alkyl complex **C**. Competing β-H/β-D elimination and statistical formation of [Pd−H]/[Pd−D] species accounts for later scrambling of deuterium at C3 and C1. Finally, a crossover experiment was conducted with an equimolar mixture of dideuterated substrate **2u**-d_2 and nondeuterated alcohol **2o** (Figure 3d). ^{2}H NMR analysis of the crude mixture showed significant incorporation of deuterium at C3 but no measurable incorporation at C2 in aldehyde **3o**-d_n. This implies that the [Pd−H] species decoordinates from the substrate only after complete conversion to the carbonyl product but not at the enol stage. The lower deuterium incorporation at C3 for **3u**-d_n compared with **3o**-d_n indicates a higher rate of isomerization of substrate **2u**-d_2 (see the SI). Finally, additional control experiments also indicated that no exchange involving the hydroxyl proton occurs during or after catalysis (see the SI).[23]

The potential decoordination of the catalyst during isomerization is a fundamental aspect of chain-walking processes. Isomerization of (*S*)-citronellol (**4r**) and its secondary alcohol analogue (4*S*)-**4s** were conducted using our optimized protocol (Scheme 5). The corresponding carbonyl derivatives **5r** and **5s**

Scheme 5. Isomerization of Citronellol Derivatives[a]

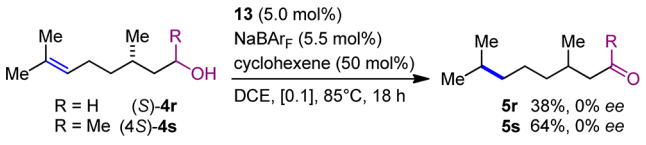

[a]Reactions were performed on a 0.25 mmol scale. Isolated yields and ee's determined by chiral HPLC or GC are shown.

were obtained in 38% and 64% yield, respectively, but in racemic form in both cases. These results indicate that the catalyst disengages from the substrate during the isomerization process. This is in contrast with previous observations. Using [Fe(CO)$_5$] as an alkene-zipper catalyst, Stockis and co-workers found that partial epimerization of **4r** and complete racemization of **4s** occur under thermal reaction conditions.[24] More recently, Sigman and co-workers convincingly established that during redox-relay Heck reactions with alkenyl alcohols, the putative [(N,N)Pd−H]$^+$ intermediate does not dissociate from the substrate upon iterative migration along the alkyl chain.[16] We believe that this result may provide an opportunity for the development of chiral catalysts for imparting stereocontrol on pre-existing stereocenters in racemic mixtures.

Enantioselective Catalysis. To evaluate the possibility of developing an enantioselective variant of these isomerization reactions, complex **15** was prepared using (*R*,*R*)-*i*-Pr-DUPHOS, a ligand that we anticipated may share electronic and steric similarities with dcpe (Scheme 6). When the reaction

Scheme 6. Enantioselective Isomerizations[a]

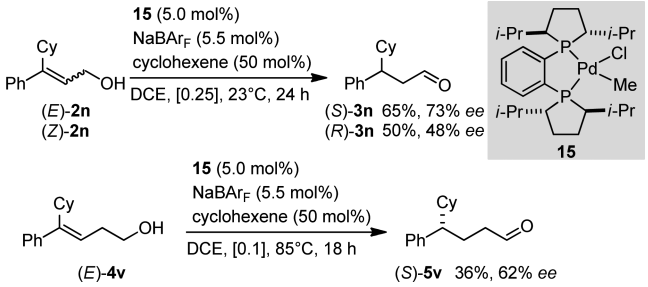

[a]Reactions were performed on a 0.25 mmol scale. Isolated yields and ee's determined by chiral HPLC are shown.

was conducted at room temperature, encouraging preliminary results were obtained for the isomerization of allylic alcohol (*E*)-**2n** and its homoallylic congener (*E*)-**4v**. The corresponding aldehydes (*S*)-**3n** and (*S*)-**5v** were isolated in 65% yield with 73% ee and in 36% yield with 62% ee, respectively. Furthermore, the reaction was found to be stereospecific because isomerization of (*Z*)-**2n** delivered (*R*)-**3n** in 50% yield with 48% ee.

Computational Investigations. To further investigate the reaction mechanism, we performed a series of density functional theory (DFT) calculations using 1,2-bis(di-*tert*-butylphosphino)ethane (dtbpe) and 1,3-bis(di-*tert*-butylphosphino)propane (dtbpp) as model ligands. Replacement of the cyclohexyl and isopropyl substituents in dcpe and dippp by *tert*-butyl groups reduces the number of conformers and has only a minor effect on the reaction profile, as was examined for the most favorable reaction pathways. This is further supported by the similar reactivities observed with [(dtbpe)Pd(Me)(Cl)] and **13** for selected substrates (see the SI for details).[27] The model palladium hydride complex **16** was used as a starting point of our investigations because its formation under the experimental conditions employed above is well-documented.[13,14]

*Isomerization of Allylic Alcohol (E)-**2a** Catalyzed by [(dtbpe)Pd−H]$^+$.* A reasonable reaction profile was calculated, and the most relevant intermediates and transition states are depicted in Figure 4. Coordination of allylic alcohol (*E*)-**2a** to **16** is an endergonic process that leads to the formation of **INT1** (ΔG_{rxn} = 14.5 kcal/mol). Subsequent migratory insertion of [Pd−H] across the double bond of the allylic alcohol occurs with a relatively low activation barrier of 1.8 kcal/mol (**INT1** → **TS1** → **INT2**). The resulting secondary alkyl-Pd intermediate **INT2** is characterized by a stabilizing agostic interaction with C3−H^a (i.e., formerly the hydride ligand).[28] This C−H bond is slightly elongated (1.18 Å), and the Pd−C2−C3−H dihedral angle is 7.1° (Figure 5).

Notably, intermediate **INT2** contains three β-hydrogens susceptible to β-hydride elimination: H^a, H^b, and H^c (Figure 5). Direct β-H elimination of H^b or H^c is not achievable because of the long Pd···H distances (3.54 and 3.37 Å, respectively) and

dx.doi.org/10.1021/ja508736u | J. Am. Chem. Soc. 2014, 136, 16882−16894

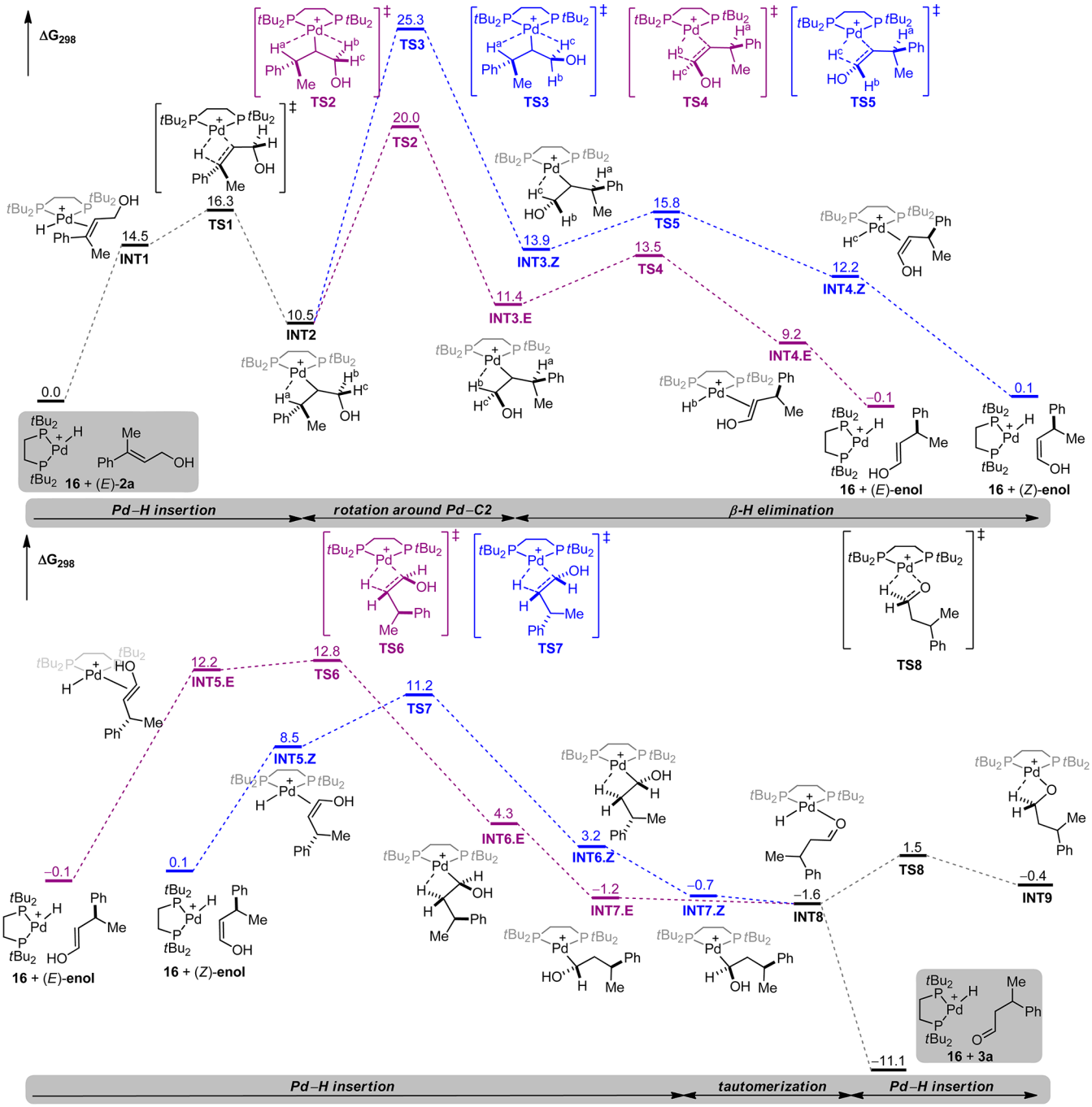

Figure 4. Computed reaction profile for the productive isomerization of (*E*)-**2a** to **3a**. The most relevant intermediates and transition states are represented. DFT method: PCM_{DCE}-B3LYP/[6-311+G(d,p); LANL2DZ]//M06L/[6-31G(d) on C, H, O, P; LANL2DZ on Pd]. Δ*G* values are given in kcal/mol.[25,26]

the large Pd−C2−C1−H dihedral angles (Pd−C2−C1−H^b = 71.2°; Pd−C2−C1−H^c = 47.5°). Rotation around the Pd−C2 bond is required in order to bring Pd−C2−C1−H^b or Pd−C2−C1−H^c into a single plane. The former rotation via **TS2** is energetically more favorable than the latter via **TS3** ($\Delta\Delta G^{\ddagger}_{TS2-TS3}$ = 5.3 kcal/mol). The resulting intermediate **INT3.E** is again stabilized by an agostic interaction (Pd−H^b = 1.92 Å; Pd−C2−C1−H = 24.2°). The Pd−C2 rotation has an activation barrier of 9.5 kcal/mol and compares well with the value computed by Wang, Wang, and co-workers for the related redox-relay Heck reaction ($\Delta G^{\ddagger}$ = 11.2 kcal/mol).[29] As a direct consequence of a switch from one agostic interaction to another, both the C−H^a and C−H^b bonds are slightly elongated in **TS2** (1.12 and 1.14 Å, respectively) (Figure 5).

Next, complex **INT3.E** undergoes β-H^b elimination via **TS4** to generate **INT4.E**, which is characterized by a π-bound (*E*)-enol. This process has a low activation barrier ($\Delta G^{\ddagger}$ = 2.1 kcal/mol). Dissociation of the (*E*)-enol from **INT4.E** is a highly exergonic process (ΔG_{rxn} = −9.3 kcal/mol). Decoordination of the (*E*)-enol from the palladium center in the sequence **INT4.E** → [**16** + (*E*)-enol] → **INT5.E** is in apparent contradiction with the results of the labeling experiments (Figure 3). Nonetheless, we also located reasonable isomeric structures of **INT5.E** in which the Pd remains on the same face of the olefin that are

dx.doi.org/10.1021/ja508736u | J. Am. Chem. Soc. 2014, 136, 16882−16894

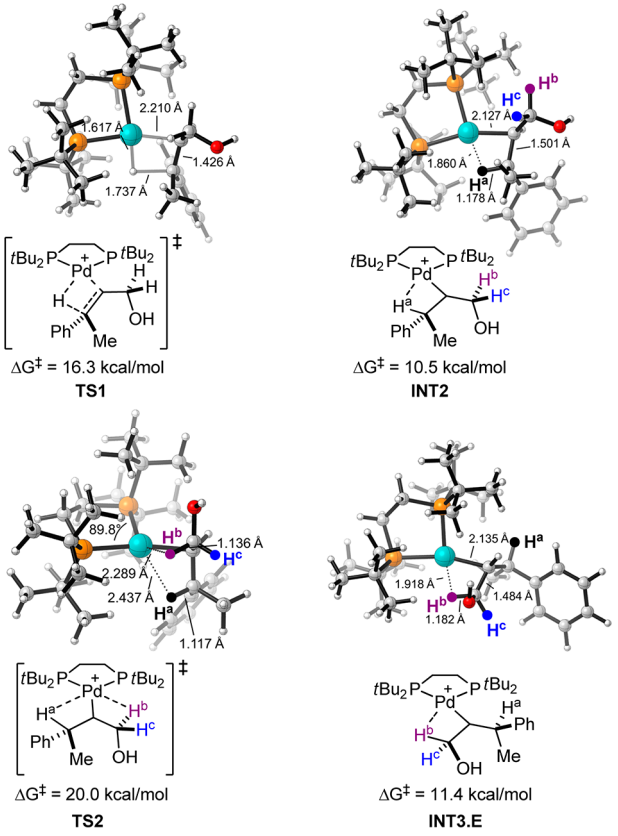

Figure 5. Most relevant intermediates and transition states in the isomerization of (*E*)-**2a**.

accessible from **INT4.E** without decoordination of the substrate (see the SI for details). Alternatively, dissociation of the enol could occur within the solvent cage and would still be consistent with the labeling studies.

The subsequent uncatalyzed tautomerization ((*E*)-enol → **3a**), although thermodynamically favorable (ΔG_{rxn} = −11.0 kcal/mol), is kinetically not feasible because the six-membered transition state of the bimolecular process lies far higher in energy than other stationary points of the reaction profile ($\Delta G^{‡}$ = 41.6 kcal/mol; see the SI). The palladium-catalyzed tautomerization pathway we computed compares more favorably (Figure 4, bottom profile). Migratory insertion of [Pd−H] across the C═C bond of the (*E*)-enol via the sequence **INT5.E** → **TS6** → **INT6.E** is a kinetically favorable exergonic process ($\Delta G^{‡}$ = 0.6 kcal/mol, ΔG_{rxn} = −7.9 kcal/mol) in which intermediate **INT6.E** is stabilized by an agostic interaction (Pd−H = 2.02 Å; Pd−C1−C2−H = 21.4°). Rotation around the Pd−C1 bond leads to the more stable coordinatively unsaturated palladium complex **INT7.E** (Pd···O = 2.26 Å, P_{trans}−Pd−C1 = 162.8°), which undergoes tautomerization to generate the product-bound palladium hydride complex **INT8**. Unfortunately, we were not able to locate a reasonable transition state for this elementary step.[16c,27] Final decoordination of [Pd−H] liberates aldehyde **3a**, which is 11.1 kcal/mol more stable than the initial allylic alcohol (*E*)-**2a**. This high exergonicity constitutes the driving force for the isomerization process.

The postreaction [Pd−H] insertion across the C═O bond of aldehyde **3a** from **INT8** was also computed. It proceeds via **TS8** and generates **INT9**. The low activation barrier of this process ($\Delta G^{‡}$ = 3.1 kcal/mol) is in full agreement with the labeling experiments of Figure 3, where scrambling of the deuterium label at C1 position was observed.

In summary, rotation around the Pd−C2 bond is turnover-determining in the isomerization of allylic alcohol (*E*)-**2a** catalyzed by $[(dtbpe)Pd–H]^{+}$ (via **TS2**). The activation free energy of 20.0 kcal/mol is also in good agreement with the experimental reaction conditions (typically, *T* = 85 °C).

*Isomerization of Allylic Alcohol (Z)-**2a** Catalyzed by [(dtbpe)Pd−H]⁺.* To understand the influence of the substrate geometry on the isomerization of allylic alcohols, we computed the reaction profile using (*Z*)-**2a** as the substrate (Figure 6). Migratory insertion of [Pd−H] into the C═C bond has a similar activation barrier as in the case of (*E*)-**2a** (16.1 vs 16.3 kcal/mol, respectively). Rotation around the Pd−C2 bond proceeds with a much lower activation barrier than for the

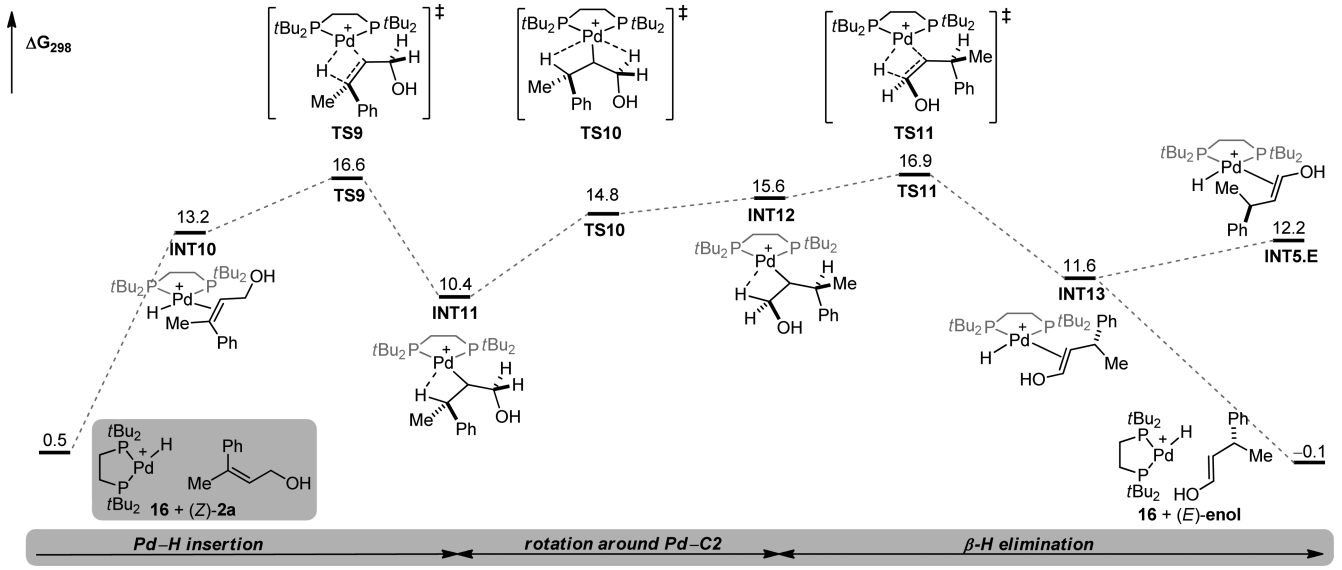

Figure 6. Computed reaction profile for the isomerization of (*Z*)-**2a** to **3a**. The most relevant intermediates and transition states are depicted. Δ*G* values are given in kcal/mol.

dx.doi.org/10.1021/ja508736u | J. Am. Chem. Soc. 2014, 136, 16882−16894

isomerization of (*E*)-**2a** (4.4 vs 9.5 kcal/mol, respectively). A comparative analysis of the two transition states reveals a strong steric interaction between the *tert*- butyl substituent of the ligand and the phenyl group of the substrate (C−H distance = 2.60 Å) in **TS2**, whereas the orientation of the smaller methyl group of the substrate toward the ligand backbone has a less destabilizing influence in **TS10** (C−H distance = 2.65 Å) (Figure 7).

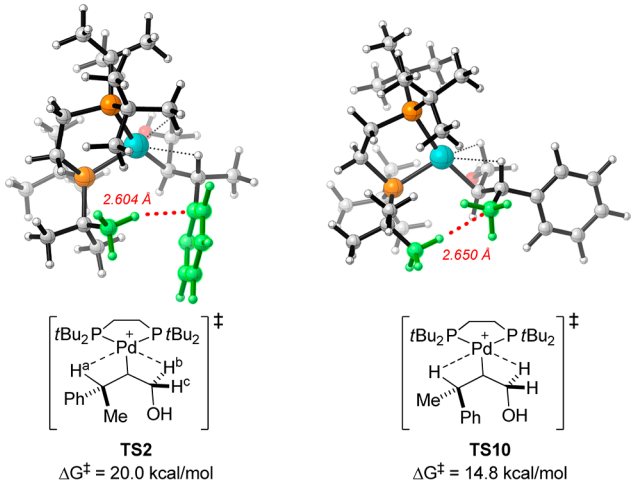

Figure 7. Structural comparison of the TSs for the Pd−C rotations in the isomerizations of (*E*)-**2a** (**TS2**) and (*Z*)-**2a** (**TS10**).

Subsequent *β*-H elimination via **TS11**, which is a facile process (activation barrier $\Delta G^{\ddagger}$ = 1.3 kcal/mol), generates the *π*-bound (*E*)-enol cationic complex **INT13**. As discussed above, this can either decoordinate in an exergonic process ([**16** + (*E*)-enol]; ΔG_{rxn} = −11.7 kcal/mol) or, in agreement with the labeling studies, directly convert to **INT5.E** without substrate dissociation (ΔG_{rxn} = 0.6 kcal/mol) (vide supra).

In summary, isomerization of (*Z*)-**2a** has a lower activation barrier than isomerization of (*E*)-**2a** (16.4 vs 20.0 kcal/mol, respectively). This is in perfect agreement with the result of monitoring experiments where (*Z*)-**2a** was found to react slightly faster than (*E*)-**2a** (see the SI). Whereas rotation around the Pd−C2 bond is rate-determining in the isomerization of (*E*)-**2a**, *β*-H elimination via **TS11** has the highest energy in the isomerization of (*Z*)-**2a**.

Competing Pathways in the Isomerization of Allylic Alcohol (E)-2a. We experimentally found that isomerization of (*E*)-**2a** to aldehyde **3a** was potentially accompanied by the formation of the terminal homoallylic alcohol **4a** and the isomeric allylic alcohol (*Z*)-**2a** (Scheme 1 and Table 1). Because the reaction is stereospecific and in view of the future development of a highly enantioselective version of this process, we sought to gain insight into the factors influencing the site selectivity in the migratory insertion of [Pd−H] across the C=C bond (Figure 8).

Coordination of (*E*)-**2a** to **16** leading to **INT14** is slightly more demanding than the binding leading to its regioisomer **INT1** (18.0 vs 14.5 kcal/mol, respectively). Migratory insertion into the double bond via **TS12** requires a very low activation energy ($\Delta G^{\ddagger}$ = 0.6 kcal/mol), although the overall activation barrier for this sequence ($\Delta G^{\ddagger}$ = 18.6 kcal/mol; Figure 8) is higher than the corresponding barrier for the regioisomeric pathway via **TS1** ($\Delta G^{\ddagger}$ = 16.3 kcal/mol; Figure 4). This difference is attributable to the increased steric interaction between the C3 substituents and the ligand backbone, as reflected by the longer Pd−C3 distance in **TS12** (2.36 Å; Figure 9) compared with the Pd−C2 distance in **TS1** (2.21 Å; Figure 5).

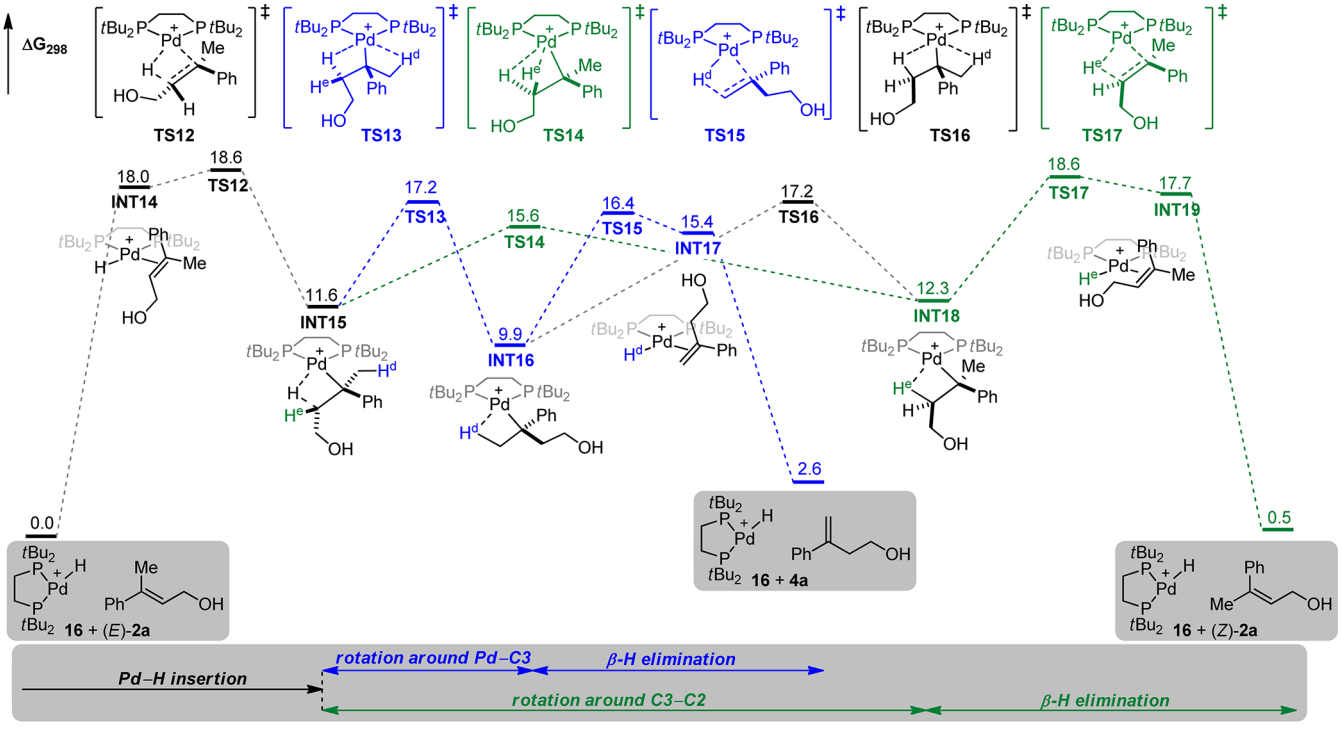

Figure 8. Computed reaction profile for the competing isomerization processes: (*E*)-**2a**/(*Z*)-**2a**, (*E*)-**2a**/**4a**, and (*Z*)-**2a**/**4a**. The most relevant intermediates and transition states are depicted. Δ*G* values are given in kcal/mol.

dx.doi.org/10.1021/ja508736u | J. Am. Chem. Soc. 2014, 136, 16882−16894

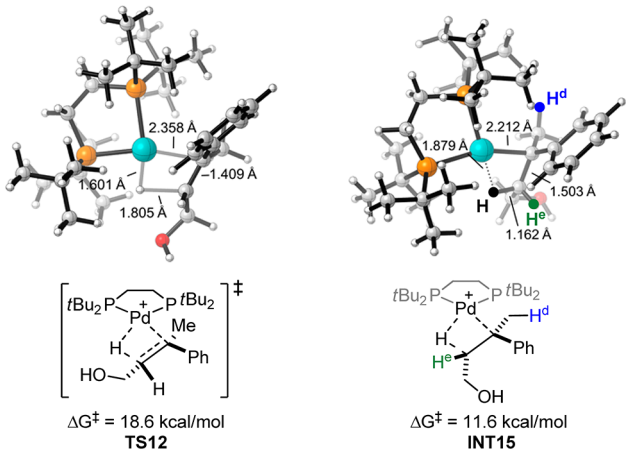

Figure 9. Most relevant intermediates and transition states in the competing isomerization processes.

Rotation around the Pd−C3 single bond in **INT15** via **TS13** proceeds with a low barrier ($\Delta G^{\ddagger}$ = 5.6 kcal/mol) and generates intermediate **INT16**, which is characterized by an agostic interaction between the Pd atom and one C−H^{d} bond of the methyl group (blue pathway). Subsequent β-H elimination via **TS15** ($\Delta G^{\ddagger}$ = 6.5 kcal/mol) affords **INT17** and is followed by dissociation of the terminal homoallylic alcohol **4a**. The overall process (*E*)-**2a** → **4a** is slightly endergonic (ΔG_{rxn} = 2.6 kcal/mol) (Figure 8).

Alternatively, rotation around C3−C2 in intermediate **INT15** (**INT15** → **TS14** → **INT18**; $\Delta G^{\ddagger}$ = 4.0 kcal/mol) poises one of the two diastereotopic hydrogen atoms (H^{e}) in a favorable position for subsequent β-H elimination (green pathway). This elementary step has an activation barrier of 6.3 kcal/mol and produces complex **INT19** with the *Z*-configured allylic alcohol. Decoordination of the substrate is exergonic, and there is no significant thermodynamic preference for one allylic alcohol isomer over the other. Overall, the isomerization of allylic alcohol (*E*)-**2a** to either **4a** or (*Z*)-**2a** presents a lower activation barrier than the productive isomerization leading to aldehyde **3a** shown in Figure 4 (18.6 vs 20.0 kcal/mol, respectively). These computational results are not fully consistent with the labeling experiments conducted with (*E*)-**2a**, where no D incorporation on the methyl substituent was detected (Figure 3b). Although the activation energy of the competing processes might be underestimated, the drastically different result obtained in the isomerization of (*E*)-**2a** with **1** suggests that subtle variations in either the ligand design or the reaction conditions may dramatically impact the outcome of the isomerization reaction. Similarly, substrates with bulkier substituents at C3 may favor productive isomerization over other competing processes. Importantly, the thermodynamic sink constituted by the productive isomerization of (*E*)-**2a** to **3a** acts as a strong driving force for the whole process.

*Isomerization of Homoallylic Alcohols (E)-**4c** and (E)-**4l** Catalyzed by [(dtbpe)Pd−H]$^{+}$.* Because of the strong influence of the olefinic substitution pattern on the isomerization of homoallylic alcohols, the reaction profiles for the isomerization of homoallylic alcohols (*E*)-**4c** and (*E*)-**4l** catalyzed by [(dtbpe)Pd−H]$^{+}$ were computed. The reaction profile for the isomerization of (*E*)-**4c** is similar to that for the isomerization of (*E*)-**2a**, and the most significant portion is displayed in Figure 10 (see the SI for the complete reaction profile). While coordination of homoallylic alcohol (*E*)-**4c** to [Pd−H] is slightly more favorable than coordination of allylic alcohol (*E*)-**2a** (13.4 vs 14.5 kcal/mol), the subsequent migratory insertion across the C═C bond in (*E*)-**4c** proceeds with a higher

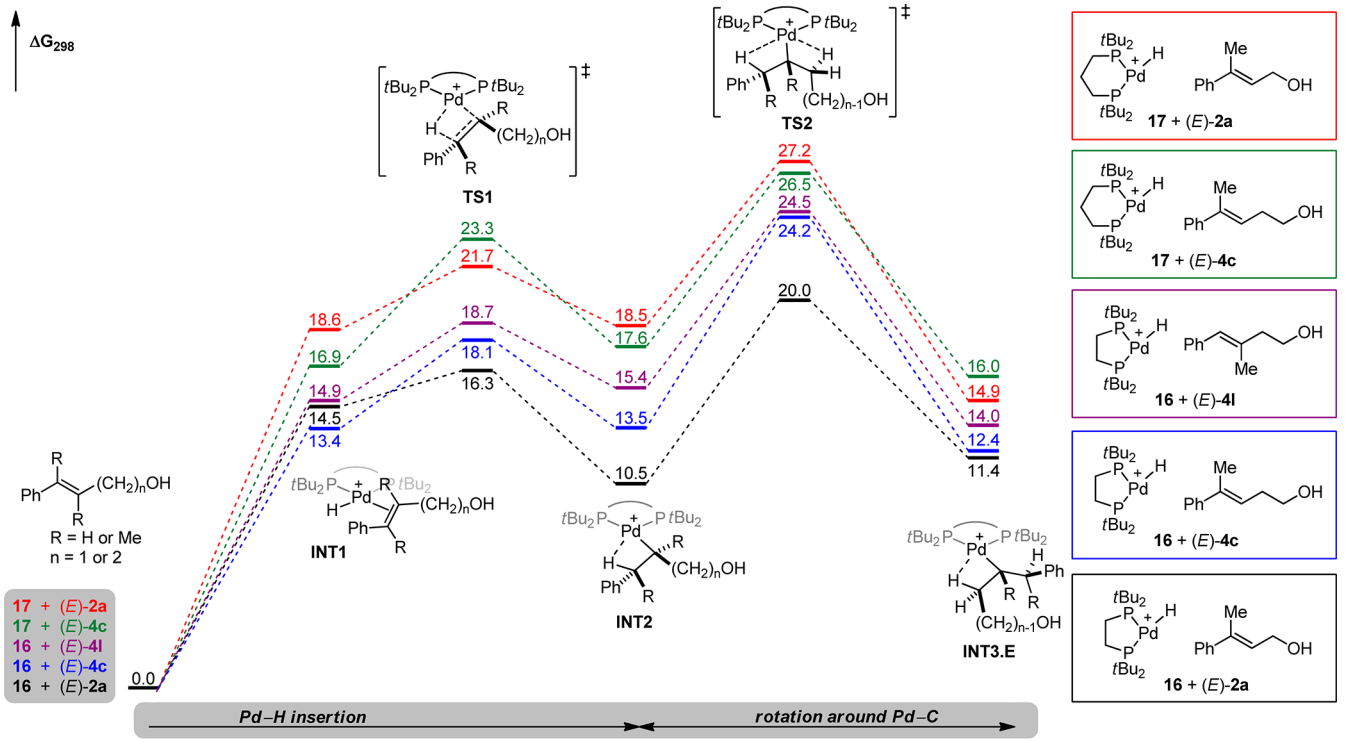

Figure 10. Comparative and partial representation of the computed reaction profiles for the isomerizations of (*E*)-**2a**, (*E*)-**4c**, and (*E*)-**4l** with the model catalysts **16** and **17**. ΔG values are given in kcal/mol.

dx.doi.org/10.1021/ja508736u | J. Am. Chem. Soc. 2014, 136, 16882−16894

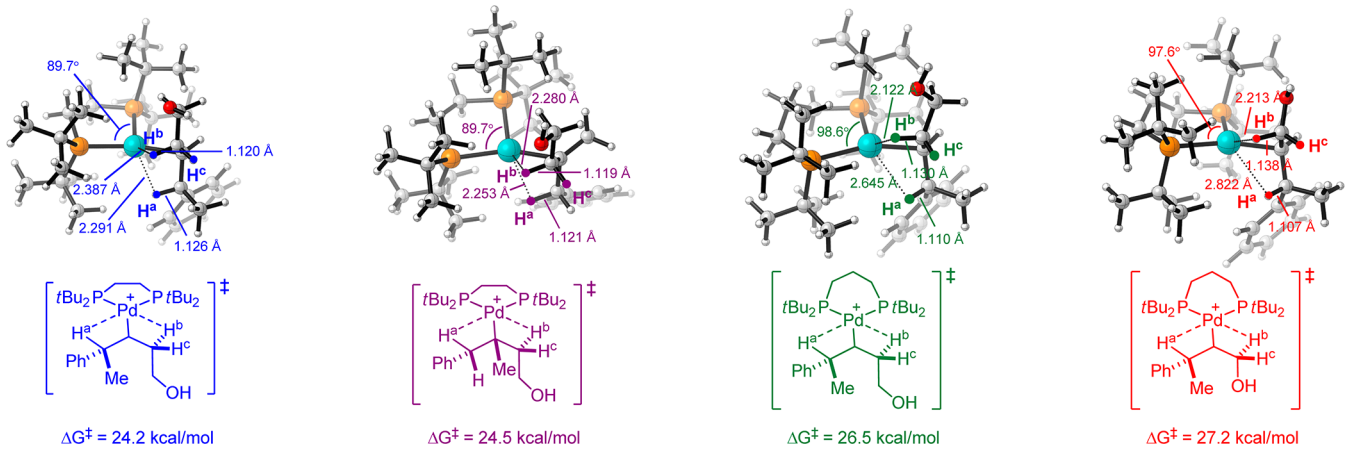

Figure 11. Comparative structural analysis of the turnover-determining transition state (**TS2**) in the isomerizations of (*E*)-**2a**, (*E*)-**4c**, and (*E*)-**4l** with model catalysts **16** and **17**. The color code is the same as the one used in Figure 10.

activation barrier (18.1 vs 16.3 kcal/mol, respectively). For the isomerization of homoallylic alcohol (*E*)-**4c**, **INT2**, **TS2**, and **INT3.E** are higher in energy than the corresponding stationary points for the isomerization of allylic alcohol (*E*)-**2a**. More importantly, the transition state corresponding to the rotation around the newly formed Pd−C bond is rate-determining in both cases (compare the blue and black lines in Figure 10: 24.2 vs 20.0 kcal/mol for **TS2**). Inspection of the respective molecular structures of **TS2** reveals that the Pd−H^a distance is shorter than the Pd−H^b distance for the isomerization of (*E*)-**4c** (2.29 vs 2.39 Å; Figure 11), whereas Pd−H^a is longer than Pd−H^b for the isomerization of (*E*)-**2a** (2.44 vs 2.29 Å; Figure 5). These computational results are in line with the experimental data, where homoallylic alcohols with this olefinic substitution pattern displayed a lower reactivity compared with the analogous allylic alcohols (Schemes 3 and 4).

The overall reaction profile for the isomerization of (*E*)-**4l** is similar to that of (*E*)-**4c**. The activation free energies of the turnover-determining transition state **TS2** are very close (24.5 vs 24.2 kcal/mol, respectively; compare the blue and purple lines in Figure 10). The structural parameters of **TS2** are also very similar for the two alcohols (Figure 11). At first sight, the computational results may not properly reflect the experimental data, as 3,3,4-trisubstituted homoallylic alcohols delivered the carbonyl derivatives in higher yields than their 3,4,4-trisubstituted analogues. Nonetheless, consumption of the starting material proceeded with similar efficiencies in these two cases, but the isomerization of 3,4,4-trisubstituted homoallylic alcohols was accompanied by the formation of additional side products.[20]

*Isomerizations of (E)-**2a** and (E)-**4c** Catalyzed by [(dtbpp)Pd−H]$^+$.* To get a better understanding of the influence of the ligand structure on the isomerization of allylic and homoallylic alcohols, the reaction profiles for the isomerizations of the structurally related allylic and homoallylic alcohols (*E*)-**2a** and (*E*)-**4c** were also computed using [(dtbpp)Pd−H]$^+$ (**17**) as a model for catalyst **1** or **7**. For the sake of clarity, the results for the [Pd−H] insertion/rotation sequence are also summarized in Figure 10 (green and red lines; see the SI for the complete profiles).

The coordination of either substrate to the coordinatively unsaturated complex [(P,P)Pd−H]$^+$ (i.e., the formation of **INT1**) is clearly a less favorable process when dtbpp is employed as a ligand (compare the black line with the red line and the blue line with the green line in Figure 10; $\Delta\Delta G_{rxn}$ = 4.1 kcal/mol for (*E*)-**2a** and 3.5 kcal/mol for (*E*)-**4c**). This is a direct consequence of the wider bite angle of dtbpp with respect to dtbpe (105.9° in **17** vs 92.3° in **16**, respectively) which imposes a stronger steric interaction between the P substituents and the substrate substituents.[19,30] The free energies of the turnover-determining **TS2** are also higher with the dtbpp ligand ($\Delta G^{\ddagger}$ = 26.5 kcal/mol for (*E*)-**4c** and $\Delta G^{\ddagger}$ = 27.2 kcal/mol for (*E*)-**2a**). Interestingly, we found large variations in the bite angles of the chelating bisphosphine ligand in **17** and **TS2** for dtbpp (**17** → **TS2**: 105.9° → 97.6° for (*E*)-**2a**). In contrast, dtbpe adopts a more rigid conformation (**16** → **TS2**: 92.3° → 89.7° for (*E*)-**2a**). These observations may account for the difference in reactivity between the catalysts supported by dcpe and dippp ligands. Overall, these computational results are also in agreement with the lower reactivity of (*E*)-**4c** in the isomerization reaction catalyzed by complex **1** or **7**. Similarly, the isomerization of (*E*)-**2a** catalyzed by [(dtbpe)-Pd−H]$^+$ is more favorable than that catalyzed by [(dtbpp)Pd−H]$^+$ ($\Delta\Delta G^{\ddagger}$ = 7.2 kcal/mol). This again reflects the experimental results obtained for this allylic alcohol (Scheme 1 and Table 1).

As a final complementary note, we never observed coordination of the hydroxyl functionality to the Pd atom throughout the computed reaction profiles of the productive isomerization of either the allylic alcohols or the homoallylic alcohols investigated.

CONCLUSION

We have discovered a readily accessible palladium catalyst that isomerizes a variety of allylic, homoallylic, and alkenyl primary and secondary alcohols into the corresponding carbonyl derivatives. To the best of our knowledge, this is the first example of an isomerization catalyst that bridges the gap between allylic and alkenyl alcohols as well as between primary and secondary substrates. The system operates under relatively mild conditions, tolerates a number of potentially reactive functional groups, and—more importantly—is virtually insensitive to the number, position, and nature of the substituents of the olefinic moiety. The preliminary results obtained for the enantioselective isomerization of a handful of substrates augur well for the development of a more general asymmetric version of these isomerization reactions.

dx.doi.org/10.1021/ja508736u | J. Am. Chem. Soc. 2014, 136, 16882−16894

The results of a combined experimental and theoretical mechanistic study are in support of a chain-walking process that operates by iterative migratory insertion/β-H elimination sequences for both allylic and homoallylic alcohols. The irreversible nature of the first migratory insertion across the C═C bond constitutes one of the key features of the proposed mechanism. The rotation around the newly formed Pd−C bond was identified as the turnover-determining step for the productive isomerization of *E*-configured substrates. This process has markedly lower activation energy for the isomerization of (*Z*)-allylic alcohols. A postreaction insertion of [Pd−H] across the C═O bond of the carbonyl products has been identified experimentally and reproduced in silico. Interestingly, we found experimentally that the catalyst does not dissociate from the substrate in the isomerization of allylic alcohols, whereas it disengages during the isomerization of alkenyl alcohols when an additional substituent is present on the alkyl chain. Finally, the effect of the bite angle of the chelating bisphosphine ligand on the catalyst activity has been well-reproduced computationally. This subtle structural change may be important for the development of improved generation of achiral and chiral catalysts.

■ ASSOCIATED CONTENT

Ⓢ Supporting Information

Experimental procedures, spectral data and crystallographic data (CIF) for complexes **11** (CCDC 1020394) and **13** (CCDC 1020782), computational data, and full ref 24. This material is available free of charge via the Internet at http://pubs.acs.org.

■ AUTHOR INFORMATION

Corresponding Author

clement.mazet@unige.ch

Notes

The authors declare no competing financial interest.

■ ACKNOWLEDGMENTS

This work was supported by the University of Geneva and Roche. We thank Prof. Tomasz A. Wesolowski and Dr. Amalia Poblador-Bahamonde (University of Geneva) for offering us access to their computational facilities. We thank Dr. Céline Besnard (University of Geneva) for assistance with X-ray diffraction measurements and crystal structure resolution. All of the molecular structures were generated using CYLview.[31] One referee is acknowledged for suggesting important control labeling experiments.

■ REFERENCES

(1) (a) Anastas, P. T.; Warner, J. C. *Green Chemistry: Theory and Practice*; Oxford University Press: New York, 1998. (b) Sheldon, R. A.; Arends, I.; Hanefeld, U. *Green Chemistry and Catalysis*; Wiley-VCH: Weinheim, Germany, 1997. (c) Anastas, P.; Eghbali, N. *Chem. Soc. Rev.* **2010**, *39*, 301.

(2) (a) Trost, B. M. *Science* **1991**, *254*, 1471. (b) Trost, B. M. *Angew. Chem., Int. Ed. Engl.* **1995**, *34*, 259. (c) Wender, P. A.; Verma, V. A.; Paxton, T. J.; Pillow, T. H. *Acc. Chem. Res.* **2008**, *41*, 40. (d) Wender, P. A.; Miller, B. L. *Nature* **2009**, *460*, 197. (e) Burns, N. Z.; Baran, P. S.; Hoffmann, R. W. *Angew. Chem., Int. Ed.* **2009**, *48*, 2854.

(3) (a) *Comprehensive Asymmetric Catalysis*; Jacobsen, E. N., Pfaltz, A., Yamamoto, H., Eds.; Springer: Berlin, 1999; Vols. *1*−*3*. (b) Walsh, P. J.; Kozlowski, M. C. *Fundamentals of Asymmetric Catalysis*; University Science Books: Sausalito, CA, 2009. (c) Hoveyda, A. H.; Evans, D. A.; Fu, G. C. *Chem. Rev.* **1993**, *93*, 1307. (d) Mahatthananchai, J.; Dumas, A. M.; Bode, J. W. *Angew. Chem., Int. Ed.* **2012**, *51*, 10954.

(4) (a) Trost, B. M.; Toste, F. D.; Pinkerton, A. B. *Chem. Rev.* **2001**, *101*, 2067. (b) Yue, C. J.; Liu, Y.; He, R. *J. Mol. Catal. A: Chem.* **2006**, *259*, 17.

(5) (a) van der Drift, R. C.; Bouwman, E.; Drent, E. *J. Organomet. Chem.* **2002**, *650*, 1. (b) Uma, R.; Crévisy, C.; Grée, R. *Chem. Rev.* **2003**, *103*, 27. (c) Kuźnik, N.; Krompiec, S. *Coord. Chem. Rev.* **2007**, *251*, 222. (d) Krompiec, S.; Krompiec, M.; Penczek, R.; Ignasiak, H. *Coord. Chem. Rev.* **2008**, *252*, 1819. (e) Aubert, C.; Fensterbank, L.; Garcia, P.; Malacria, M.; Simonneau, A. *Chem. Rev.* **2011**, *111*, 1954. (f) Mantilli, L.; Mazet, C. *Chem. Lett.* **2011**, *40*, 341. (g) Ahlsten, N.; Bartoszewicz, A.; Martin-Matute, B. *Dalton Trans.* **2012**, *41*, 1660.

(6) Seminal contribution: (a) Kumobayashi, H.; Akutagawa, S.; Otsuka, S. *J. Am. Chem. Soc.* **1978**, *100*, 3949. For recent reviews, see: (b) Akutagawa, S. In *Comprehensive Asymmetric Catalysis*; Jacobsen, E. N., Pfaltz, A., Yamamoto, H., Eds.; Springer: Berlin, 1999; Vol. *2*, Chapter 23, pp 813−832. (c) Akutagawa, S. In *Comprehensive Asymmetric Catalysis*; Jacobsen, E. N., Pfaltz, A., Yamamoto, H., Eds.; Springer: Berlin, 1999; Vol. *3*, Chapter 41.1, pp 1461−1472. (d) Fu, G. C. In *Modern Rhodium-Catalyzed Organic Reactions*; Evans, P. A., Ed.; Wiley-VCH: Weinheim, Germany, 2005; Chapter 4, pp 79−91.

(7) (a) Tanaka, K.; Qiao, S.; Tobisu, M.; Lo, M. M.-C.; Fu, G. C. *J. Am. Chem. Soc.* **2000**, *122*, 9870. (b) Tanaka, K.; Fu, G. C. *J. Org. Chem.* **2001**, *66*, 8177. For a related contribution, see: (c) Chapuis, C.; Barthe, M.; de Saint Laumer, J.-Y. *Helv. Chim. Acta* **2001**, *84*, 230.

(8) (a) Mantilli, L.; Mazet, C. *Tetrahedron Lett.* **2009**, *50*, 4141. (b) Mantilli, L.; Gérard, D.; Torche, S.; Besnard, C.; Mazet, C. *Angew. Chem., Int. Ed.* **2009**, *48*, 5413. (c) Mantilli, L.; Mazet, C. *Chem. Commun.* **2010**, *46*, 445. (d) Mantilli, L.; Gérard, D.; Torche, S.; Besnard, C.; Mazet, C. *Chem.—Eur. J.* **2010**, *16*, 12736. (e) Mantilli, L.; Gérard, D.; Besnard, C.; Mazet, C. *Eur. J. Inorg. Chem.* **2012**, 3320. (f) Li, H.; Mazet, C. *Org. Lett.* **2013**, *15*, 6170. For other work using iridium, see: (g) Li, J.-Q.; Peters, B.; Andersson, P. G. *Chem.—Eur. J.* **2011**, *17*, 11143.

(9) (a) Arai, N.; Sato, K.; Azuma, K.; Ohkuma, T. *Angew. Chem., Int. Ed.* **2013**, *52*, 7500. For related contributions, see: (b) Sun, Y.; LeBlond, C.; Wang, J.; Blackmond, D. G.; Lauirada, J.; Sowa, J. R., Jr. *J. Am. Chem. Soc.* **1995**, *117*, 12647. (c) Bizet, V.; Pannecoucke, X.; Renaud, J.-L.; Cahard, D. *Angew. Chem., Int. Ed.* **2012**, *51*, 6467. (d) Wu, R.; Beauchamps, M. G.; Laquidara, J. M.; Sowa, J. R., Jr. *Angew. Chem., Int. Ed.* **2012**, *51*, 2106.

(10) (a) Kitamura, M.; Manabe, K.; Noyori, R. *Tetrahedron Lett.* **1987**, *28*, 4719. (b) Hiroya, K.; Kurihara, Y.; Ogasawara, K. *Angew. Chem., Int. Ed. Engl.* **1995**, *34*, 2287. (c) Ito, M.; Kitahara, S.; Ikariya, T. *J. Am. Chem. Soc.* **2005**, *127*, 6172. (d) Fernández-Zúmel, M. A.; Lastra-Barreira, B.; Scheele, M.; Díez, J.; Crochet, P.; Gimeno, J. *Dalton Trans.* **2010**, *39*, 7780.

(11) (a) Grotjahn, D. B.; Larsen, C. R.; Gustafson, J. L.; Nair, R.; Sharma, A. *J. Am. Chem. Soc.* **2007**, *129*, 9592. For related studies from the same group, see: (b) Larsen, C. R.; Grotjahn, D. B. *J. Am. Chem. Soc.* **2012**, *134*, 10357. (c) Erdogan, G.; Grotjahn, D. B. *Org. Lett.* **2014**, *16*, 2818. For a related study, see: (d) Ishibashi, K.; Takahashi, M.; Yokota, Y.; Oshima, K.; Matsubara, S. *Chem. Lett.* **2005**, *34*, 664.

(12) For a general review of palladium hydrides, see: (a) Grushin, V. V. *Chem. Rev.* **1996**, *96*, 2011. For important contributions on Pd-catalyzed isomerization processes, see: (b) Ionescu, A.; Ruppel, M.; Wendt, O. F. *J. Organomet. Chem.* **2006**, *691*, 3806. (c) Coquerel, Y.; Brémond, P.; Rodriguez, J. *J. Organomet. Chem.* **2007**, *692*, 4805. (d) Lim, H. J.; Smith, C. R.; RajanBabu, T. V. *J. Org. Chem.* **2009**, *74*, 4565. (e) Gauthier, D.; Lindhardt, A. T.; Olsen, E. P. K.; Overgaard, J.; Skrydstrup, T. *J. Am. Chem. Soc.* **2010**, *132*, 7998. (f) Sabitha, G.; Nayak, S.; Bhikshapathi, M.; Yadav, J. S. *Org. Lett.* **2011**, *13*, 382. For a related account, see: (g) Widenhoefer, R. A. *Acc. Chem. Res.* **2002**, *35*, 905.

(13) (a) Johnson, L. K.; Killian, C. M.; Brookhart, M. *J. Am. Chem. Soc.* **1995**, *117*, 6414. (b) Johnson, L. K.; Mecking, S.; Brookhart, M. *J. Am. Chem. Soc.* **1996**, *118*, 267. (c) Guan, Z.; Cotts, P. M.; McCord, E. F.; McLain, S. J. *Science* **1999**, *283*, 2059. (d) Berkefeld, A.; Mecking,

S. *Angew. Chem., Int. Ed.* **2006**, *45*, 6044. (e) Okada, T.; Park, S.; Takeuchi, D.; Osakada, K. *Angew. Chem., Int. Ed.* **2007**, *46*, 6141. (f) Okada, T.; Takeuchi, D.; Shishido, A.; Ikeda, T.; Osakada, K. *J. Am. Chem. Soc.* **2009**, *131*, 10852. (g) Guan, Z. *Chem.—Asian J.* **2010**, *5*, 1058. (h) Takeuchi, D. *J. Am. Chem. Soc.* **2011**, *133*, 11106. (i) Okada, T.; Park, S.; Takeuchi, D.; Osakada, K. *Angew. Chem., Int. Ed.* **2007**, *46*, 6141. For noncatalytic long-range isomerization, see: (j) Chinkov, N.; Levin, A.; Marek, I. *Angew. Chem., Int. Ed.* **2006**, *45*, 465. (k) Chinkov, N.; Levin, A.; Marek, I. *Synlett* **2006**, 501.

(14) Kochi, T.; Hamasaki, T.; Aoyama, Y.; Kawasaki, J.; Kakiuchi, F. *J. Am. Chem. Soc.* **2012**, *134*, 16544.

(15) Ohlmann, D. M.; Tschauder, N.; Stockis, J.-P.; Gooßen, K.; Dierker, M.; Gooßen, L. J. *J. Am. Chem. Soc.* **2012**, *134*, 13716.

(16) (a) Werner, E. W.; Mei, T.-S.; Burckle, A. J.; Sigman, M. S. *Science* **2012**, *338*, 1455. (b) Mei, T.-S.; Werner, E. W.; Burckle, A. J.; Sigman, M. S. *J. Am. Chem. Soc.* **2013**, *135*, 6830. (c) Xu, L.; Hilton, M. J.; Zhang, X.; Norrby, P.-O.; Wu, Y.-D.; Sigman, M. S.; Wiest, O. *J. Am. Chem. Soc.* **2014**, *136*, 1960. (d) Mai, T.-S.; Patel, H. H.; Sigman, M. S. *Nature* **2014**, *508*, 340.

(17) Vyas, D. J.; Larionov, E.; Besnard, C.; Guénée, L.; Mazet, C. *J. Am. Chem. Soc.* **2013**, *135*, 6177.

(18) Larionov, E.; Li, H.; Mazet, C. *Chem. Commun.* **2014**, *50*, 9816.

(19) (a) Raebiger, J. W.; Miedaner, A.; Curtis, C. J.; Miller, S. M.; Anderson, O. P.; DuBois, D. L. *J. Am. Chem. Soc.* **2004**, *126*, 5502. (b) Morris, R. H. *J. Am. Chem. Soc.* **2014**, *136*, 1948. (c) Bullock, R. M.; Appel, A. M.; Helm, M. L. *Chem. Commun.* **2014**, *50*, 3125.

(20) The main component was identified as a dimerization product reminiscent of those observed by Ryu and co-workers: Doi, T.; Fukuyama, T.; Minamino, S.; Husson, G.; Ryu, I. *Chem. Commun.* **2006**, 1875. See the Supporting Information for additional details.

(21) Ishibashi, K.; Matsubara, S. *Chem. Lett.* **2007**, *36*, 724.

(22) The slight variations between the extent of D incorporation and the initial catalyst loading are within the experimental margin of error (ca. 1%).

(23) The imperfect balance of D incorporation at C2 in the experiments of Figure 3c,d is not due to competing tautomerization reactions involving the starting allylic alcohol, enol intermediates, and/or the final aldehyde. Indeed, mixing **3u**-d_n with **2o** under the reaction conditions for catalysis did not change the extent of D incorporation at C2. Similar results were obtained in the absence of the Pd catalyst. See the SI for details.

(24) Weissberger, E.; Stockis, A.; Carr, D. D.; Giebfried, J. *Bull. Soc. Chim. Belg.* **1980**, *89*, 281.

(25) Frisch, M. J.; et al. *Gaussian 09*, revision A.02; Gaussian, Inc.: Wallingford, CT, 2009.

(26) (a) For the LANL2 effective core potential, see: Hay, P. J.; Wadt, W. R. *J. Chem. Phys.* **1985**, *82*, 270. (b) For the PCM solvation model, see: Tomasi, J.; Mennucci, B.; Cammi, R. *Chem. Rev.* **2005**, *105*, 2999.

(27) To further validate the use of dtbpe as a model for dcpe, this noncommercial ligand was synthesized according to the following literature procedure: Scherer, W.; Herz, V.; Brück, A.; Hauf, C.; Reiner, F.; Altmannshofer, S.; Leusser, D.; Stalke, D. *Angew. Chem., Int. Ed.* **2011**, *50*, 2845. The corresponding complex [(dtbpe)Pd(Me)(Cl)] was evaluated for the isomerization of representative model substrates (**2a**, **2b**, **2h**, **2m**, and **4c**) and provided yields similar to those obtained with **13** under the prototypical reaction conditions for isomerization (62%, 89%, 79%, 58%, and 44% respectively). See the SI for details.

(28) (a) Scherer, W.; McGrady, G. S. *Angew. Chem., Int. Ed.* **2004**, *43*, 1782. (b) Brookhart, M.; Green, M. L. H.; Parkin, G. *Proc. Natl. Acad. Sci. U.S.A.* **2007**, *104*, 6908.

(29) Dang, Y.; Qu, S.; Wang, Z.-X.; Wang, X. *J. Am. Chem. Soc.* **2014**, *136*, 986.

(30) (a) Dierkes, P.; van Leeuwen, P. W. N. M. *J. Chem. Soc., Dalton Trans.* **1999**, 1519. (b) van Leeuwen, P. W. N. M.; Kamer, P. C. J.; Reek, J. N. H.; Dierkes, P. *Chem. Rev.* **2000**, *100*, 2741. (c) Kamer, P. C. J.; van Leeuwen, P. W. N. M.; Reek, J. N. H. *Acc. Chem. Res.* **2001**, *34*, 895.

(31) Legault, C. Y. *CYLview*, version 1.0.561b; Université de Sherbrooke: Sherbrooke, QC, 2014; http://www.cylview.org